Engineering Applications of Artificial Intelligence 133 (2024) 108084

Contents lists available at ScienceDirect

Engineering Applications of Artificial Intelligence

journal homepage: www.elsevier.com/locate/engappai

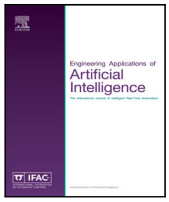

Research paper

Unmanned Aerial Vehicle-enabled grassland restoration with energy-sensitive of trajectory design and restoration areas allocation via a cooperative memetic algorithm

Dongbin Jiao [a,b], Lingyu Wang [a], Peng Yang [b,c,*], Weibo Yang [d], Yu Peng [a], Zhanhuan Shang [e], Fengyuan Ren [a]

[a] School of Information Science and Engineering, Lanzhou University, Lanzhou, 730000, P.R. China
[b] Guangdong Provincial Key Laboratory of Brain-inspired Intelligent Computation, Department of Computer Science and Engineering, Southern University of Science and Technology, Shenzhen, 518055, P.R. China
[c] Department of Statistics and Data Science, Southern University of Science and Technology, Shenzhen, 518055, P.R. China
[d] School of Automobile, Chang'an University, Xi'an, 710064, P.R. China
[e] State Key Laboratory of Grassland Agro-Ecosystem, College of Ecology, Lanzhou University, Lanzhou, 730000, P.R. China

ARTICLE INFO

Keywords:
Grassland restoration
Unmanned Aerial Vehicle (UAV)
Trajectory design
Restoration area
Cooperative memetic algorithm
Decomposition

ABSTRACT

Grassland restoration is a crucial method for preventing ecological degradation in grasslands. Unmanned Aerial Vehicles (UAVs) offer a promising solution to reduce extensive human labor and enhance restoration efficiency, given their fully automatic capabilities, yet their full potential remains exploited. This paper progresses this emerging technology for planning the grassland restoration. We undertake the first attempt to mathematically model the UAV-enabled restoration process as the maximization of restoration areas problem (MRAP). This model considers factors including limited UAV battery energy, grass seed weight, the number of restored areas, and their sizes. The MRAP is a composite problem involving trajectory design and area allocation, which are highly coupled and conflicting. Consequently, it requires solving two NP-hard subproblems: the variant Traveling Salesman Problem (TSP) and the Multidimensional Knapsack Problem (MKP) simultaneously. To address this complex problem, we introduce a novel cooperative memetic algorithm. The algorithm integrates an efficient heuristic algorithm, variant population-based incremental learning (PBIL), and a maximum-residual-energy-based local search (MRELS) strategy, referred to as CHAPBILM. The algorithm solves the two subproblems interlacedly by leveraging the interdependencies and inherent knowledge between them. The simulation results demonstrate that CHAPBILM successfully solves the MRAP on multiple instances in a near-optimal way. It also confirms the conflicts between trajectory design and area allocation. The effectiveness of CHAPBILM is further supported by comparisons with traditional optimization methods that do not exploit the interdependencies between the two subproblems. The proposed model and solution have the potential to be extended to other complex optimization problems in ecological protection and precision agriculture.

1. Introduction

Grasslands, which cover approximately 26% to 40% of the earth's total terrestrial surface (Chapin et al., 2013), are responsible for supporting 70% of the global agricultural area (Reynolds and Frame, 2005). They provide a wide range of both marketed and nonmarketed ecosystem services for humans (Reinermann et al., 2020), including livestock production, carbon storage, biodiversity conservation, water purification, erosion control, and recreation (Dass et al., 2018; Gibson, 2009). However, extensive degradation, attributed to human activities, climate change, invasive species, and other factors, has plagued grasslands for an extended period (Steffen et al., 2015). Grassland restoration emerges as a potent strategy to counteract ecological degradation in these areas (Török et al., 2021). Conventional restoration methods heavily rely on manual planning and planting operations, demanding significant human resources and often yielding suboptimal efficiency. What is worse, the limitations of fieldwork are currently

* Corresponding author at: Guangdong Provincial Key Laboratory of Brain-inspired Intelligent Computation, Department of Computer Science and Engineering, Southern University of Science and Technology, Shenzhen, 518055, P.R. China.
E-mail addresses: jiaodb@lzu.edu.cn (D. Jiao), lywang19@lzu.edu.cn (L. Wang), yangp@sustech.edu.cn (P. Yang), wbyang@chd.edu.cn (W. Yang), ypeng17@lzu.edu.cn (Y. Peng), shangzhh@lzu.edu.cn (Z. Shang), rfy@lzu.edu.cn (F. Ren).

https://doi.org/10.1016/j.engappai.2024.108084
Received 9 October 2022; Received in revised form 7 February 2024; Accepted 11 February 2024
Available online 15 February 2024

exacerbated due to the COVID-19 pandemic, which has presented new challenges such as budget cuts, travel restrictions, and safety concerns (Mohan et al., 2021). Hence, the development of an automated method for efficient and cost-effective grassland restoration becomes imperative.

In recent years, Unmanned Aerial Vehicles (UAVs) have emerged as indispensable and cost-efficient tools across various civilian applications (Zhao et al., 2018; Wang et al., 2019; Shakhatreh et al., 2019; Hong et al., 2021; Wang et al., 2022; Fang et al., 2023). In particular, UAVs have demonstrated superior potential in aspects of grassland ecological protection, including species composition studies (Sun et al., 2018), imagery (Blackburn et al., 2021), monitoring (Buters et al., 2019), plant diversity assessment (Librán-Embid et al., 2020), and remote sensing (Xiang et al., 2019). Inspired by this, this work investigates the practical yet automatic restoration technique: the UAV-enabled grassland restoration method. We consider a general scenario where a UAV carries grass seeding and grassland degradation information (such as degradation degree, grassland map, and degradation areas) to sow from the base station to each targeted area, and then returns to the base station. However, existing rotary-wing UAVs typically have limited battery energy and load capacity. As a result, it is impossible to restore all targeted areas by a UAV in a single trip. Moreover, recharging the battery and refilling the capacity for the next trip often takes much longer than the sowing process itself. Therefore, the challenge lies in maximizing the benefits within a single trip while considering various realistic constraints, including UAV energy, grass seeds weight, the number of restored areas, and their corresponding sizes.

To overcome this challenge, this study focuses on the maximization of restoration areas problem (MRAP) for UAV-enabled grassland restoration during a single trip. To the best of our knowledge, there is no existing work that explores such models in the context of MRAP for UAV-enabled grassland restoration method. Consequently, we formulate the MRAP as an energy-sensitive mathematical programming model. This model takes into account not only the limited battery energy and load capacity of UAV, but also the restoration cost associated with different degraded areas. Furthermore, upon further analysis, we discovered that the MRAP, when subjected to the aforementioned constraints, involves two conflicting objectives: finding the shortest flight path and optimizing the allocation of areas. In essence, the MRAP can be viewed as a composite problem that combines a trajectory design problem and an area allocation problem, both of which are closely coupled. This composite problem can be reduced to simultaneously solving two NP-hard problems: the variant Traveling Salesman Problem (TSP) and the Multidimensional Knapsack Problem (MKP). While existing methods can solve these two problems separately, they often neglect the dependence between them, potentially resulting in degraded final solutions. Therefore, it is crucial to design an effective and efficient algorithm that addresses both problems concurrently, considering their interdependencies.

Fortunately, cooperative optimization provides a solution to this problem. The basic idea behind cooperative optimization is to decompose the complicated problem into several subproblems and optimize them simultaneously (Huang, 2004). However, achieving a good combination of evolutionary search and problem-specific local search is crucial for effectively solving these subproblems. Memetic algorithms (MAs), which integrate local refinements with evolutionary search, draw inspiration from the principles of natural evolution and Dawkin's concept of a memea unit of cultural evolution capable of local refinements (Ong et al., 2010). MAs have demonstrated superior performance in tackling complex combinatorial optimization problems when compared to traditional methods. Examples include the TSP (Merz, 2000), Quadratic Assignment Problem (Merz, 2000), network embedding (Gong et al., 2020), scheduling problem (Wang and Wang, 2021), mission planning problem (Wang et al., 2015). Furthermore, cooperation refers to autonomous associations formed to meet common economic, social, and cultural needs. The success of MAs in addressing NP-hard problems through problem-specific algorithms within a memetic computing framework highlights their capability to effectively handle sophisticated problems. This motivates us to utilize a cooperative memetic algorithm to address the MRAP.

To achieve this, we decompose the MRAP into two stages: the trajectory design stage and the restoration areas allocation stage. Considering the dependence between these stages, we propose a novel cooperative memetic algorithm called CHAPBILM. This algorithm integrates an efficient heuristic algorithm with move operators to address the UAV trajectory design, and a variant of population-based incremental learning (PBIL) (Baluja, 1994) known as maximum-residual-energy-based local search (MRELS) strategy to solve the restoration areas allocation. Unlike solving the two stages separately, our approach optimizes both stages concurrently, taking into account the same constraint conditions. By doing so, we can fully consider the dependency between UAV trajectory design and restoration areas allocation. The effectiveness of our formulated model and the proposed CHAPBIL algorithm is evaluated through simulation studies conducted under various scenarios.

The main contributions of this study are summarized as follows:

1. We are the first to present the MRAP for UAV-enabled restoration method and subsequently formulate an energy-sensitive mathematical programming model for the MRAP, considering realistic constraints.
2. We decompose the MRAP into a two-stage optimization problem and propose a novel cooperative memetic algorithm, CHAPBILM, to effectively address the MRAP. CHAPBILM leverages the inherent dependencies between the two stages to optimize the problem more efficiently.
3. The simulation results demonstrate that CHAPBILM outperforms noncooperative optimization algorithms for the MRAP. This finding further validates the interdependency between UAV trajectory design and restoration areas allocation.

The rest of this work is structured as follows. Section 2 reviews the related work. Section 3 describes the system model and formulates the energy-sensitive mathematical programming model of MRAP for UAV-Enabled grassland restoration method. Section 4 proposes the novel cooperative memetic algorithm based on the efficient heuristic algorithm and the variant of PBIL tailored the MRAP. Section 5 demonstrates the results of simulation studies. Finally, Section 6 concludes this work.

2. Related work

Although UAV-enabled technologies have attracted widespread attention for their applications in grassland ecological protection, there is still few work on UAV seeding specifically for grassland restoration. In the following section, we provide a summary of the research closely related to our study. We begin by reviewing general models related to the UAV-enabled grassland restoration model and subsequently focus on solutions to two-stage problems.

2.1. UAV-enabled techniques

UAVs have been employed in various applications, including the creation of re-seeding maps, rather than seeding for crop production (Pedersen et al., 2017). Elliott (2016) explores the use of low-cost UAVs for automating accelerated natural regeneration through aerial seeding in tropical forest ecosystems. Huang et al. (2020) propose a specific UAV seeding system for rapeseed, which incorporates a miniature air-assisted centralized metering device. Faiçal et al. (2017) develop a system that dynamically plans flight routes to ensure precise pesticide deposition on target areas. Guo et al. (2021) present a spray distribution model and coverage path planning for spraying UAVs, with simulation results demonstrating their effectiveness. However, it is

Table 1
Meanings of the notations.

Notation	Meaning
Q	The total weight of the grass seeds carried by the UAV.
Q_i	The weight of grass seeds which restore σ_i unit circles in the ith restored area.
E_{max}	The battery capacity of UAV.
l_i	The degree of grassland degradation in the ith restored area.
q_i	The weight of grass seeds which restore per unit area in the ith restored area.
$\bar{q}_{ij}$	The weight of grass seeds carried by UAV from the restored area v_i to v_j.
σ_i	The number of unit circles restored by UAV in the ith restored area.
e_i	The energy consumption per unit area of UAV seeding in the ith restored area.
η	The positive parameter with energy consumption.
γ	The positive parameter with grassland environment.
e_{ap}	The energy consumption of UAV carrying the hyper-spectral camera for aerial photography in each unit circle σ_i.
e_{ij}^f	The energy consumption per unit distance of UAV from the restored areas v_i to v_j.
d_{ij}	The distance between the restored areas v_i and v_j.

important to note that these mentioned works typically utilize regular field maps and do not specifically consider the energy consumption of UAVs. Moreover, they often overlook path planning in conjunction with seeding, which may limit their real-world applicability.

Meanwhile, in most of the existing works on the path planning of UAV, researchers primarily focus on investigating efficient area coverage algorithms to extend the operational time of UAVs. Vasisht et al. (2017) design a novel path planning algorithm that fully utilizes wind assistance to accelerate and decelerate, thereby prolonging the UAV's operation time and minimizing the coverage duration for a given area. Palomino-Suarez and Pérez-Ruiz (2020) propose an automated workflow algorithm associated with the path planning process, which not only identifies the workspace but also handles path planning for agricultural oversight activities. Shivgan and Dong (2020) study the UAV path planning problem in environmental sensing and surveying applications. They formulate the problem as a TSP to optimize the UAV's energy and flight time. Rossello et al. (2022) tackle the challenge of covering large-scale areas in precision agriculture by developing a novel path planning algorithm for UAV. They consider the flying time constraint and aim to maximize the estimation quality of the system states. The problem is modeled as a special orienteering problem (OP), namely mixed-integer semidefinite programming (MISDP), and is solved using a heuristic algorithm. Additionally, the literature (Aggarwal and Kumar, 2020) provide a thorough survey of various path planning techniques for UAVs across different applications, while the literature (Basiri et al., 2022) focus on path planning approaches for multi-rotor UAVs in precision agriculture applications. However, it is important to note that the aforementioned studies primarily focus on single path planning without considering the simultaneous optimization of path planning and related tasks.

2.2. Two-stage optimization methods

Apart from the UAV-enabled grassland restoration model, a significant contribution of this work is the exploration of a cooperative optimization method to address the two-stage problem under specific constraints. Li et al. (2010) develop an inexact two-stage water management model for planning agricultural irrigation under uncertain conditions. Azadeh et al. (2019) propose a two-stage route optimization method to define flight boundaries and reduce the number of variables and constraints in light aircraft transport systems. Maini et al. (2019) design a two-stage strategy to find efficient solutions for cooperative route planning problems involving aerial-ground vehicles, considering fuel constraints in coverage applications. Rajan et al. (2022) formulate a two-stage stochastic program model and present a solution method for a UAV path planning problem in data gathering missions. While the aforementioned studies employ two-stage approaches to address routing planning problems, most of them decompose the problem into separate stages, solving them independently without considering the interdependencies between them and tailored solution algorithms.

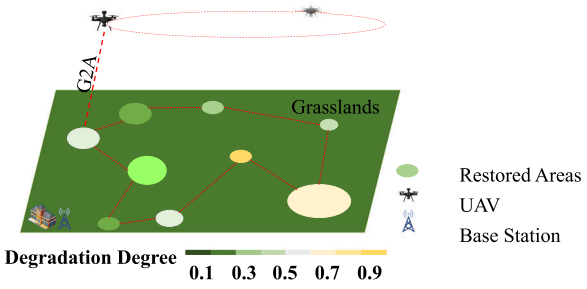

Fig. 1. An example of multi-restored areas by a UAV.

Furthermore, the bilevel programming problem (Colson et al., 2007) is another example of a two-stage optimization problem. The MRAP addressed in this work is related to the bilevel programming problem (Colson et al., 2007), which takes into account the interdependencies between the two stages of the optimization problem. Angelo and Barbosa (2015) investigate a bilevel production–distribution planning problem. Sinha et al. (2018) comprehensively review the bilevel optimization from the basic principles to the solution schemes, including classical and evolutionary methods. Feng et al. (2015) propose a memetic computational paradigm based on evolutionary optimization and transfer learning to solve routing problems. However, these approaches may not directly apply to solving the problem addressed in this work, as they do not consider the specific characteristics of the MRAP for the UAV-enabled grassland restoration method.

3. System model and problem formulation

This section first describes the UAV-enabled grassland restoration model, and then details the UAV's energy consumption model. It finally establishes the maximization of restoration areas model and formulation of the MRAP for the UAV-enabled grassland restoration method. The important parameters used in this study are summarized in Table 1, providing a reference for their notation.

3.1. UAV-enabled grassland restoration model

As shown in Fig. 1, we consider such a scenario where a UAV equipped with GPS devices, information regarding grassland degradation levels, and grass seeds. The UAV serves N restored areas on the grasslands sequentially before returning to the base station,[1] ensuring that it does not exhaust its energy supply. The UAV has a battery capacity E_{max} which is fully charged initially. Additionally, the UAV

[1] The UAV is scheduled from its depot (i.e., base station), we assume that the home service station is co-located with the base station.

carries a weight of grass seeds represented by Q. Each circular area corresponds to a degraded areas on the grasslands. Different colors are employed to indicate a score ranging from 0 to 1, representing the degree of grassland degradation. Lighter colors signify higher scores, indicating more severe degradation. In accordance with international principles and standards for ecological restoration practices (Gann et al., 2019), we stipulate that areas with scores below 0.3 can restore themselves naturally, while those above 0.8 are challenging to restore using the UAV-enabled method. It is noteworthy that areas with scores between 0.3 and 0.8 may have the potential to self-restore over time if the growth conditions are suitable for vegetation. However, the UAV-enabled method can expedite the recovery process of degraded grasslands and reduce the cost of manual restoration.

Let l_i denote the degree of grassland degradation in the ith restored area, where $l_i \in (0, 1)$. Specifically, UAV seeding can be employed to restore the degraded areas on the grasslands when the degree of grassland degradation l_i falls within the range of $[0.3, 0.8]$. Areas outside this range are not suitable for restoration via UAV seeding. However, the most significant challenge arises from the limited energy capacity of the UAV's battery, which restricts the operational time of the UAV. Additionally, besides performing seeding tasks, the UAV is also responsible for collecting restoration data from each restored area for subsequent trips. As a result, in a restoration process, it is possible to restore either a part or the entirety of each restored area through UAV seeding.

Typically, the MRAP of UAV-enabled grassland restoration method can be denoted as a fully connected weighted graph $G = (V, A)$. The vertex set $V = \{v_0, v_1, \ldots, v_N\}$ is composed by the base station v_0 and the restored area v_i, respectively. Each restored area $v_i \in V_a$, where the set $V_a = V \setminus v_0$. The arc set $A = \{(v_i, v_j) | v_i, v_j \in V, i \neq j\}$ denotes the set of the paths connecting the restored areas. Each arc $a \in A, a = (v_i, v_j)$ is associated with a non-negative value d_{ij} which denotes the distance between the restored areas v_i and v_j. The UAV starts from the base station with the weight of grass seeds Q. The total weight of grass seeds be $Q = \sum_{i=1}^{N} Q_i$. When the UAV arrives at a restored area $i \in V_a$, it needs Q_i weight of grass seeds to sow the degraded area partially or entirely. Hence, the total weight of grass seeds carried by the UAV is reduced by Q_i as it restores the degraded areas. In addition, the seed weight Q_i required for the degraded area v_i depends on both the size of restored area and the degree of grassland degradation in that specific area as determined by the UAV.

Generally speaking, the energy consumption for UAV restoration increases with the size of the restored area on the grasslands and the degree of grassland degradation. The operational time of the UAV is constrained by both its weight and the stored energy of the battery while maintaining a constant speed. In this study, a rotary-wing UAV is chosen for grassland restoration due to its ability to hover at a fixed point. Dorling et al. (2017) derive the power consumption equation for an $h-$rotor UAV as

$$P(\bar{q}_{ij}) = (M + \bar{q}_{ij})^{\frac{3}{2}} \sqrt{\frac{g^3}{2\rho\varsigma h}}, \tag{1}$$

where $M = W + m$. Here, W denotes the frame weight, m is battery weight, $\bar{q}_{ij}$ is the payload, g is the standard gravitational acceleration, ρ denotes the fluid density of air, ς denotes the area of spinning blade disc, and h denotes the number of rotors. In this work, $\bar{q}_{ij}$ denotes the weight of grass seeds carried by UAV from the restored area v_i to v_j.

Assume that the UAV flies at a fixed altitude H and a constant speed v between the restored areas. For the sake of simplicity, we neglect the influence of various weather conditions, such as temperature, wind, rain, and sandstorms, on the UAV's flight.

3.2. Energy consumption model for UAV

During a restoration process, the energy consumption in a scheduling cycle of the UAV comprises three primary components: the energy consumption of UAV seeding E_s in the restored areas, the energy consumption of UAV aerial photography E_{ap}, and the energy consumption of UAV flight E_f. Additionally, according to Dorling et al. (2017), the energy consumption of the UAV is directly proportional to the payload weight when maintaining a fixed altitude and constant speed.

3.2.1. Energy consumption for seeding

Due to the varying sizes of the restored areas and the limited seeding capacity of the UAV at each hovering point, we discretize each restored area into c_i unit circles, where $i = 1, \ldots, n$. The UAV is designed to sow grass seeds within the area of a single unit circle during each hovering point. Since the UAV must complete the seeding task in each restored area of the grasslands once and return to the base station before depleting its energy, the number of unit circles to be restored in each area depends on the UAV's current remaining energy. Additionally, the energy consumption is directly proportional to the weight of grass seeds carried by the UAV. On one hand, this implies that larger restored areas require a greater number of unit circles to be restored, resulting in higher energy consumption and the sowing of more grass seeds. On the other hand, areas with a higher degree of grassland degradation pose greater restoration challenges, necessitating a larger quantity of grass seeds and consequently increased energy consumption.

Therefore, the energy consumption of UAV seeding can be considered as a function of the degradation level and the weight of grass seeds carried by the UAV. The energy consumption per unit area of UAV seeding can be defined as

$$e_i = \eta q_i, \tag{2}$$

where η is a positive parameter with energy consumption and q_i is the weight of grass seeds to be restored per unit area in the ith restored area.

Moreover, the weight of grass seeds restored per unit area can be regarded as a function of the degree of grassland degradation in the ith restored area (Klaus et al., 2016). Specifically, it can be expressed as

$$q_i = (1 + l_i)^{\gamma}, \tag{3}$$

where $l_i \in [0.3, 0.8]$ is the degree of grassland degradation in the ith restored area and γ is a positive parameter with grassland environment. The addition of grass seed weight in different areas of grassland degradation is influenced by various factors, such as the number of grass seed species, seed mass, seed quality, seed mixing method, and the types of grassland (Bai et al., 2020; Freitag et al., 2021; Resch et al., 2022).

The weight of grass seeds that restore σ_i unit circles in the ith restored area can be denoted as

$$Q_i = \sigma_i q_i, \tag{4}$$

where σ_i denotes the number of the unit circles restored by UAV in the ith restored area. It is subject to the condition $1 \leq \sigma_i \leq c_i$ and $l_i \in [0.3, 0.8]$, signifying that the UAV restores either a partial or the entire degraded area in the ith restored area during the restoration process.

Therefore, the total energy consumption by UAV seeding in the restored areas can be expressed as

$$E_s = \sum_{i=1}^{N} \sum_{j \neq i}^{N} \sigma_i e_i x_{ij}, \tag{5}$$

where the binary variables x_{ij} determine whether or not the UAV will service the restored area j. More specifically, x_{ij} equals 1 if the UAV flies from the restored area i to j, and 0 otherwise.

3.2.2. Energy consumption for aerial photography

In addition to seeding, UAV also play a crucial role in collecting restoration information for each restored area, which helps facilitate the next restoration efforts.

The total energy consumption of UAV carrying the hyper-spectral camera for aerial photography can be expressed as

$$E_{ap} = e_{ap} \sum_{i=1}^{N} \sum_{j \neq i}^{N} x_{ij} \sigma_i, \tag{6}$$

where e_{ap} denotes the energy consumption of the UAV carrying the hyper-spectral camera for aerial photography in each unit circle σ_i restored by the UAV. This energy consumption is independent of the grassland degradation degree but depends on the number of unit circles σ_i restored in each area.

3.2.3. Energy consumption for flight

The energy consumption during UAV flight encompasses three components: the energy consumed by the UAV when flying from the base station to the restored areas, the energy consumed during UAV flight between two adjacent restored areas, and the energy consumed when the UAV returns to the base station after servicing each restored area. Let $x_{ij} \in \{0, 1\}$ denote the binary decision variables, defining as

$$x_{ij} = \begin{cases} 1, & (v_i, v_j) \text{ is covered in the tour,} \\ 0, & \text{otherwise.} \end{cases} \tag{7}$$

As the UAV maintains a fixed altitude H and constant speed v, the energy consumption per unit distance remains consistent. Thus, the total energy consumption during UAV flight in a restoration process can be expressed as

$$E_f = \sum_{i=0}^{N} \sum_{j \neq i}^{N} e_{ij}^{f} d_{ij} x_{ij}, \tag{8}$$

where e_{ij}^{f} denotes energy consumption per unit distance of the UAV.

The energy consumption per unit distance of the UAV, considering the seed weight $\bar{q}_{ij}$ combined with Eq. (1), can be expressed as

$$e_{ij}^{f} = P(\bar{q}_{ij}) = (M + \bar{q}_{ij})^{\frac{3}{2}} \sqrt{\frac{g^3}{2\rho\varsigma h}}, \tag{9}$$

where $\bar{q}_{ij}$ denotes the weight of the grass seeds carried by the UAV from the restored area v_i to v_j, satisfying

$$\sum_{j=0, i \neq j}^{N} \bar{q}_{ji} - \sum_{j=0, i \neq j}^{N} \bar{q}_{ij} = Q_i, \forall i \in V_a, \tag{10}$$

$$\bar{q}_{ij} \leq Q x_{ij}, \forall (i, j) \in A. \tag{11}$$

3.3. Maximization of restoration areas model

Due to the limited battery energy and load capacity of the UAV, it is not possible to restore all degraded areas on the grasslands in a single restoration process. Therefore, our objective is to restore as much of the grassland degradation areas as possible while adhering to the energy constraints imposed by the UAV-enabled method. It means that the effort to maximize the sum of each restored area σ_i, considering the degree of grassland degradation $l_i \in [0.3, 0.8]$. This objective can be expressed as

$$C = \sum_{i=1}^{N} \sigma_i, \tag{12}$$

where C denotes the maximum sum of the number of unit circles to be restored after the UAV has serviced all restored areas in a restoration process.

3.4. Problem formulation

This paper considers the MRAP for the UAV-enabled grassland restoration method. The objective is to maximize restoration areas C after the UAV has serviced all restored areas in a restoration process. The problem involves optimizing the energy consumption of seeding and aerial photography within the restored areas, as well as determining the UAV's flight trajectory while considering practical constraints of the UAV and the grassland degradation. The problem can be formulated as

$$\max_{x_{ij}, \sigma_i} \quad C = \sum_{i=1}^{N} \sum_{j \neq i}^{N} x_{ij} \sigma_i \tag{13a}$$

$$s.t. \quad \sum_{i=1}^{N} \sum_{j \neq i}^{N} \sigma_i e_i x_{ij} + e_{ap} \sum_{i=1}^{N} \sum_{j \neq i}^{N} x_{ij} \sigma_i + \sum_{i=0}^{N} \sum_{j \neq i}^{N} (M + \bar{q}_{ij})^{\frac{3}{2}} \times \sqrt{\frac{g^3}{2\rho\varsigma h}} x_{ij} d_{ij} \leq E_{max}, \tag{13b}$$

$$\sum_{i=1, i \neq j}^{N} \sigma_i q_i x_{ij} \leq Q, \forall j \in V_a, \tag{13c}$$

$$\sum_{j=0, i \neq j}^{N} \bar{q}_{ji} - \sum_{j=0, i \neq j}^{N} \bar{q}_{ij} = \sigma_i q_i, \quad \forall i \in V_a, \tag{13d}$$

$$\bar{q}_{ij} \leq Q x_{ij}, \quad \forall (i, j) \in A, \tag{13e}$$

$$\sum_{i=0, i \neq j}^{N} x_{ij} = \sum_{j=0, i \neq j}^{N} x_{ij} = 1, \quad \forall i, j \in V_a, \tag{13f}$$

$$\sum_{j=1}^{N} x_{0j} = \sum_{j=1}^{N} x_{j0} = 1, \tag{13g}$$

$$x_{ij} \in \{0, 1\}, \tag{13h}$$

$$1 \leq \sigma_i \leq c_i, \tag{13i}$$

$$\bar{q}_{ij} \geq 0. \tag{13j}$$

Constraints (13b) ensure that the energy consumption in a scheduling cycle of UAV cannot exceed its energy capacity E_{max}. Constraints (13c) enforce that the weight of the grass seeds Q carried by UAV must be sowed before the UAV returns to the base station. Constraints (13d) indicate the reduced weight of grass seeds for UAV after it severs a restored area and meets the demanded for that area, while also eliminating any illegal sub-tours. Constraints (13e) guarantee that the demanded grass seeds at the restored area v_j cannot exceed the weight of remaining grass seeds carried by the UAV. Constraints (13f) ensure that the UAV enters each restored area at most once and leaves the restored area after seeding. Constraints (13g) guarantee that the UAV begins and ends its route at the base station. Constraint (13h) ensures that the binary variables value are integers. Constraint (13i) ensures that the number of unit circles to be restored does not exceed the maximum areas. Constraint (13j) is nonnegativity restrictions.

The optimization problem (13) is a multi-variable combinatorial optimization problem, since the set of feasible solutions is discrete in terms of the binary variable x_{ij} and the integer variable σ_i. Therefore, it is difficult to directly solve the optimization problem (13) by using the traditional optimization methods. By further analyzing, we can find the following characteristics. Firstly, the size of restoration areas and the amount of seeding in each area may vary depending on the UAV's service order and flight trajectory. Secondly, the size of restoration areas and seeding amounts have an impact on the subsequent UAV flight trajectory. In essence, the trajectory design of the UAV, the size of restoration areas, and the amount of seeding are closely coupled.

If the optimization problem (13) is solved directly, these factors are generated separately, disregarding their interdependence. Therefore, there exist two challenges for solving effectively the optimization problem (13).

1. Can the multi-variable combinatorial optimization problem be solved easily in other forms?
2. How can we effectively consider the interdependence among the UAV trajectory design, restoration area sizes, and seeding quantities?

4. Cooperative memetic algorithm for MRAP

This section first presents the problem decomposition and the related challenges. It then describes the framework of the cooperative memetic algorithm, CHAPBILM, specifically designed for addressing the UAV-enable grassland restoration problem. Finally, it provides a detailed explanation of the solution to the two-stage problem after the decomposition process.

4.1. Problem decomposition

To tackle the challenges outlined above, we address them by decomposing the optimization problem (13) into a two-stage optimization problem. More specifically, the first stage focuses on the trajectory design of the UAV, while the second stage involves the processes of seeding and aerial photography.

In the first stage, the UAV needs to determine the restored areas for grass seed sowing, aiming to maximize the restoration area and minimize energy consumption within each area. Since the distances between restored areas v_i and v_j are different, there may have different degrees of grassland degradation l_i and l_j, the number of the unit circles restored σ_i and σ_j, and the weight of demanded grass seeds Q_i and Q_j. The sequence in which the restored areas are selected can lead to different total energy consumption and total restoration areas C. Consequently, the trajectory design of the UAV poses a typical combinatorial optimization problem, resembling the TSP. This problem is known to be NP-hard, as acknowledged by Chiang et al. (2019), making the selection of the optimal flight trajectory a challenging task. While exact algorithms can find the optimal solution, they often entail high computational costs, particularly for large-scale problems. Furthermore, the optimal flight trajectory of the UAV is influenced by the process of seeding and aerial photography. As the energy consumption of the UAV is affected by the size of the restored area, these factors exhibit interdependencies and can mutually impact each other.

In the second stage, the UAV carries out grass seed sowing and aerial photography in the selected restored area. However, due to the UAV's limited energy capacity, it is possible that some restored areas cannot be fully restored in a single restoration process. Additionally, the UAV needs to gather restoration data through aerial photography for subsequent restoration efforts, requiring each restored area to have at least one unit area sown. As a result, it becomes essential to dynamically determine the number of unit circles to be restored in each area, with the objective of maximizing the total restoration area C. This restoration areas allocation problem can also be considered a typical combinatorial optimization problem, analogous to the MKP (Kellerer et al., 2004). Specifically, the restored areas V_a can be regarded as a set of items. The number of the unit circles restored σ_i by the UAV, and the total number of the unit circles restored c_i in the ith restored area can be regarded as the profit and capacity at the ith resource, respectively. The UAV's battery capacity E_{max} can be equated to the capacity of the knapsack. The goal is to find a set of the items that yield the maximum value (i.e., maximum total restoration areas C), while adhering to the battery capacity constraint of the UAV. However, the distinction between our model and the MKP lies in the fact that in the MKP, each item can be selected or not, whereas in our model, it is mandatory for each restored area to have at least one unit area restored.

Although the optimization problem (13) has been decomposed into two stages to enhance clarity and facilitate comprehension, there are two significant challenges that need to be taken into account:

1. How can the two stages be effectively dealt with simultaneously, ensuring that the optimization problem (13) is solved without disregarding their interdependency?
2. How can a strategy be designed to accelerate the optimization process?

4.2. Cooperative memetic algorithm based on a heuristic algorithm and variant PBIL with local search

To address the aforementioned challenges, we propose a novel cooperative memetic algorithm called CHAPBILM. This algorithm is specifically designed to efficiently address the MRAP for UAV-enabled grassland restoration. The fundamental principle of the cooperative memetic algorithm involves decomposing the complex problem into simpler sub-problems. These sub-problems are then optimized simultaneously within a cooperative memetic computing framework, under consistent conditions such as shared parameters and variables (Wang and Wang, 2021). This makes the cooperative memetic algorithm well-suited for handling the decomposed two-stage optimization problem.

In this paper, the cooperative memetic algorithm aims to simultaneously optimize the UAV's flight trajectory in the first stage and the number of restored unit circles in the second stage, so as to maximize the total of restoration areas C during the restoration process. The general framework of CHAPBILM is presented in Algorithm 1. The parameters of the optimization problem (13) and the cooperative memetic algorithm are first input in the initialization phase, respectively (line 2). Subsequently, a feasible initial solution is generated for the optimization problem. A greedy heuristic is employed to design the UAV trajectory, improving a given flight trajectory of the UAV while adhering to the specified constraints. Meanwhile, a possible restoration area vector is generated, satisfying the constraints and corresponding to the designed UAV trajectory (lines 5–6). The optimal trajectory $\mathbf{V}^*$ is selected from the generated paths, and the optimal restoration areas $\mathbf{\Sigma}^*$ is obtained from the possible allocation areas (lines 8–9). The algorithm then enters the cooperative optimization phase. In the first stage, the UAV trajectory is designed using a heuristic algorithm with move operators under the given constraints (line 12). In the second stage, the variant of the PBIL algorithm is employed to determine the optimal restoration area associated with the designed UAV trajectory (line 13). The performance of the UAV trajectory design and its corresponding optimal restoration areas is evaluated (line 14). A local search strategy, MRELS, is applied to enhance the current solution and expedite convergence (line 16). Finally, the global optimal UAV trajectory and the optimal restoration areas are updated (lines 17–18). This process continues until the termination criteria are met, and the algorithm returns the optimal UAV trajectory and the corresponding optimal restoration areas.

In the subsequent sections, we will provide a detailed description of the cooperative memetic algorithm, which is based on an efficient heuristic algorithm and a variant of PBIL with the MRELS strategy. This algorithm is specifically designed to solve the MRAP.

4.3. First stage: Trajectory design for UAV

The objective of the UAV trajectory design is to optimize the restored order of the areas under realistic constraints related to the UAV and grassland degradation. This optimization aims to maximize the total restoration areas of all the restored areas.

To improve the flight trajectory of the UAV during a restoration process, the embedded Greedy_Heuristic_Algorithm sub-procedure in Algorithm 2 employs traditional move operators (Bräysy and Gendreau, 2005; Liu et al., 2021), including *2-opt*, *or-opt*, *swap*, and *inversion*. Fig. 2 illustrates the effects of these move operators on a given UAV trajectory. In the illustration, the circles represent restored areas, and the red dashed boxes depict the results before and after applying the move operations.

Algorithm 1: The General Framework of CHAPBILM for MRAP

Input: The restored areas v_i, the degree of grassland degradation $l_i \in (0,1)$, the restored area c_i, the total weight of the grass seeds Q, the neighborhood size of the generated path NB, and the battery capacity of UAV E_{max};
/*----------Initialization----------*/
Initialize parameters for the heuristic algorithm and the variant of PBIL;
/*----------Generate initial solution----------*/
gen = 0;
Recursively calling Greedy_Heuristic_Algorithm($\mathbf{V}$) to generate NB trajectories of UAV;
Solve the optimal restoration areas, randomly generate N possible restoration area vectors under constraints, corresponding to the UAV trajectory designed;
Compute the objection function value C;
$\mathbf{V}^* \leftarrow$ Select_Best_Trajectory $(v_1, v_2, \ldots, v_N)$;
$\mathbf{\Sigma}^* \leftarrow$ Select_Best_Area $(\sigma_1, \sigma_2, \ldots, \sigma_N)$;
/* - Optimal restoration areas based on the heuristic algorithm and the variant of PBIL - */
while $gen < gen_{max}$ **do**
  Recursively calling Greedy_Heuristic_Algorithm($\mathbf{V}$) to generate NB trajectories of UAV;
  Solve the optimal restoration area via the variant of PBIL algorithm, corresponding to the UAV trajectory designed;
  Evaluate the total restoration areas C with the corresponding optimal restored area in each restored area;
  Select the best-so-far UAV trajectory and the optimal number of unit circles in each restored area according to the total restoration areas C;
  Perform the local research strategy MRELS on the best-so-far solution $\tilde{\mathbf{V}}, \tilde{\mathbf{\Sigma}}$;
  $\mathbf{V}^* \leftarrow$ Select_Best_Trajectory $(\tilde{v}_1, \tilde{v}_2, \ldots, \tilde{v}_N)$;
  $\mathbf{\Sigma}^* \leftarrow$ Select_Best_Area $(\tilde{\sigma}_1, \tilde{\sigma}_2, \ldots, \tilde{\sigma}_N)$;
  $gen = gen + 1$;
end while
Output: *Optimal UAV trajectory* $\mathbf{V}^* = [v_1^*, v_2^*, \ldots, v_N^*]$, *optimal number of restored areas* $\mathbf{\Sigma}^* = [\sigma_1^*, \sigma_2^*, \ldots, \sigma_N^*]$, and optimal total restoration areas $C^*(\mathbf{V}^*, \mathbf{\Sigma}^*)$.

Algorithm 2: The Greedy Heuristic Algorithm for UAV Trajectory Design

Input: Initialize UAV trajectory $\mathbf{V} = (v_1, v_2, \ldots, v_N)$;
Output: UAV trajectory $\tilde{\mathbf{V}} = (v_1, v_2, \ldots, v_N)$;
set of move operators (N_j): *2-opt*, *or-opt*, *swap*, and *inversion*;
$j = 1$;
while $j \leq 4$ **do**
  $\tilde{\mathbf{V}} \leftarrow$ utilize move operators (N_j) on $\mathbf{V}$
  if $\tilde{\mathbf{V}}$ does not violate the energy constraints of UAV **then**
    $\mathbf{V} \leftarrow \tilde{\mathbf{V}}$;
    $j = 1$;
  else
    $j = j + 1$;
  end if
end while
return $\tilde{\mathbf{V}}$

To provide more details, the left side of each subfigure displays the initial routes, while the right side shows the results after applying the *2-opt*, *or-opt*, *swap*, and *inversion* operators, respectively. The *2-opt* operator is to invert a subsequence of two consecutive restored areas in a route as shown in Fig. 2(a). The *or-opt* operator is to remove a subsequence of one or two consecutive restored areas from the route and reinserts it into another position of the same route or different route, as shown in Fig. 2(b). The *swap* operator is to exchange a subsequence of one or two consecutive restored areas, which are on the same route but not overlapping each other, as shown in Fig. 2(c). The *inversion* operator is to convert a subsequence of two consecutive restored areas into its reverse, as shown in Fig. 2(d).

To improve a given route $\mathbf{V}$, a best-improvement search strategy is employed within its neighborhoods, which are defined by the four move operators mentioned earlier. This strategy involves evaluating all routes that can be obtained by applying any of the four operators to $\mathbf{V}$. The objective is to find the optimal feasible route among these options. In this search strategy, the route $\tilde{\mathbf{V}}$ is compared to $\mathbf{V}$. If $\tilde{\mathbf{V}}$ is deemed better than $\mathbf{V}$, considering that the total restoration areas achieved under the current route $\tilde{\mathbf{V}}$ are larger and the energy constraint of the UAV is not violated, then the route $\mathbf{V}$ is updated. This process continues until no further improvement is found. By utilizing these move operators, it is ensured that an optimal route is reached within each neighborhood.

After the UAV trajectory has been designed, the corresponding optimal restoration area is obtained in the second stage.

4.4. Second stage: Restoration areas allocation

The goal of the second stage is to optimize the number of unit circles restored in each restored area in order to maximize the total restoration areas across all restored areas, based on the UAV trajectory designed in the first stage.

As introduced in Section 4.1, it was mentioned that using an exact algorithm (Fleszar, 2022) is not a suitable choice for exploring the optimal solution to this problem. Instead, population-based stochastic algorithms, such as evolutionary algorithms (EAs) including ant colony optimization (ACO), genetic algorithm (GA), and PBIL, are commonly applied to tackle NP-hard problems (Yang et al., 2024; Fidanova, 2021; Rezoug et al., 2018; Jiao et al., 2017). In this work, the variant of PBIL is selected to optimize the number of unit circles restored in each restored area. Several reasons support this choice, which are enumerated as follows.

1. The MRAP discussed in this paper is a combinatorial optimization problem that can be seen as a particular MKP, and PBIL has been shown successful application in solving such kind of problems (Wang et al., 2012).
2. Compared with other EAs, PBIL has neither cross operation nor mutation operation, and adopts an explicit probability model to guide sampling for the promising candidate solutions. Although the exact number of unit circles to be restored in each restored area is not known in advance, their probability can be obtained through the learning mechanism in PBIL.

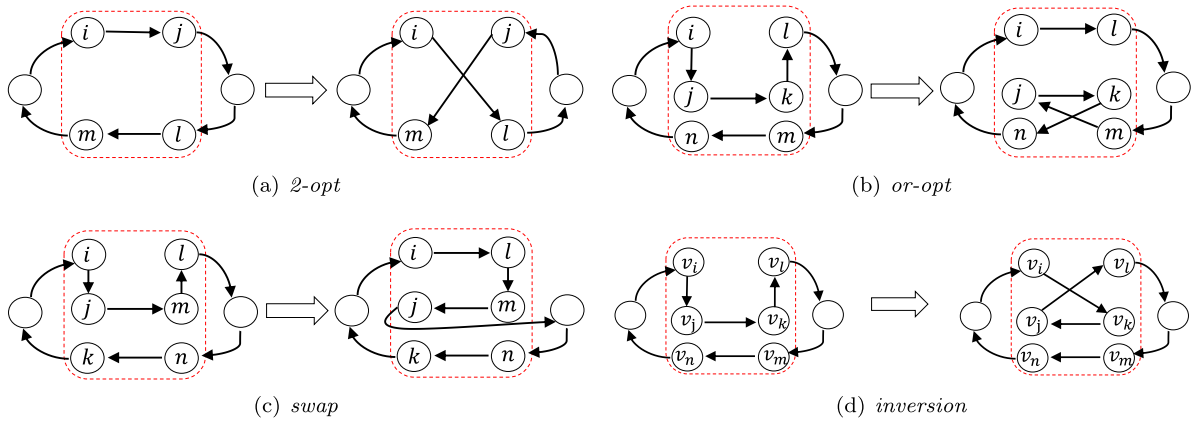

Fig. 2. Illustrative of move operators utilized: *2-opt*, *or-opt*, *swap*, and *inversion*. (a) The *2-opt* operator inverts a subsequence of two consecutive restored areas v_i and v_j in a route. (b) The *or-opt* operator removes a subsequence of two consecutive restored areas v_i and v_k from the route and reinserts it between v_l and v_n in the same route. (c) The *swap* operator exchanges the positions of the restored areas v_j and v_l in a route. (d) The *inversion* operator converts a subsequence of two consecutive restored areas v_j and v_k in a route into its reverse.

These advantages may make PBIL more suitable for solving the restoration areas allocation problem. In this study, PBIL consists of four components: (1) restoring areas representation; (2) fitness evaluation; (3) probability model and updating mechanism; (4) local search strategy.

4.4.1. Restoring areas representation

In this study, it is essential for the UAV to determine the appropriate number of unit circles to be restored in each restored area, taking into account the constraints and the UAV trajectory designed. Therefore, we adopt a real vector $\mathbf{\Sigma}$ to represent the number of unit circles restored in all restored areas, where $\mathbf{\Sigma} = [\sigma_1, \ldots, \sigma_n], \sigma_i \in [1, c_i]$. It is important to note that there is a one-to-one correspondence between the number of unit circles restored σ_i, and the sequence of UAV trajectory. This implies that each different trajectory sequence vector $\mathbf{V}$ corresponds to a distinct restored area vector $\mathbf{\Sigma}$.

4.4.2. Fitness evaluation

The performance of a solution, which consists of a UAV trajectory sequence and its corresponding optimal restoration areas, can be evaluated using a fitness function. However, it is challenging to ensure that all degradation areas can be restored within the constraints of limited energy and grass seed weight during the restoration process. Some restored areas may not have any feasible candidate solutions under these conditions. Consequently, these areas cannot be fully restored in the process, indicating the potential absence of a feasible solution for the optimization problem (13). To address this issue, the approach taken is to first design a UAV trajectory sequence and then maximize the total number of unit circles restored in the areas. Therefore, a fitness function is proposed to evaluate the performance of solutions.

$$F(v, \sigma^*) = \sum_{i=1}^{N} \sum_{j \neq i}^{N} x_{ij} \sigma_j^*. \tag{14}$$

4.4.3. Probability model and updating mechanism

In PBIL, the probability model serves to describe the distribution of the solution space and is typically constructed based on the specific characteristics of the problem being solved. In this work, we utilize a probability matrix $\mathbf{P}$ as the probability model, specifically tailored to the optimization of the restoration area problem. The probability matrix $\mathbf{P}$ can be defined as

$$\mathbf{P} = [p_{ij}]_{M \times N}, \tag{15}$$

where $p_{ij} = \frac{1}{\sigma_{ij}}$, $i \in M, j \in N$, denoted by the number of unit circles restored σ_j in the ith restored area seeded by the UAV during the restoration process. Generally, the elements in probability matrix $\mathbf{P}$ are initialized as $p_{ij}(0) = \frac{1}{c_{ij}}$, $i \in M, j \in N$, which means that the solution space can be sampled uniformly in the initialization phase.

At the end of each generation, a new solution is generated using the roulette strategy, which samples the search space guided by the probability matrix $\mathbf{P}$. To explore promising areas effectively, the probability model needs to be improved through an updating mechanism. The updating mechanism consists of two main steps. Firstly, a superior sub-population is determined using the tournament selection strategy. This sub-population comprises the best SP solution, where $SP = \theta \cdot P, \theta \in (0, 1)$. The selection process prioritizes solutions with higher fitness, ensuring that superior solutions have a greater influence on the probability model. Secondly, the probability model is updated by incorporating historical knowledge and statistical information from the superior sub-population. The probability matrix updates are based on the following Hebbian-inspire rule

$$p_{ij}(g+1) = (1-\alpha) p_{ij}(g) + \alpha \frac{1}{N} \sum_{k=1}^{N} x_{ij}^k, \tag{16}$$

where $\alpha \in (0, 1)$ is the learning rate, indicating that the proportion of historical information selected by children's generation $g+1$ from their parents' generation g, and x_{ij}^k is the kth solution of the superior sub-population in the gth generation.

4.4.4. Maximum-residual-energy-based local search

After evaluating the fitness function, if the *Select-Best-Solution* $\{\mathbf{V}^*, \mathbf{\Sigma}^*\}$ is a feasible solution, a maximum-residual-energy-based local search (MRELS) strategy is performed on it to accelerate the convergence. It is important to note that altering the UAV trajectory sequence may lead to changes in the number of unit circles to be restored, consequently affecting the total restored areas in the restoration process. Additionally, the degradation level directly impacts the number of unit circles the UAV can seed in each restored area, with a proportional relationship denoted by $\sigma_i \propto \frac{1}{l_i}$. Moreover, due to the UAV's limited energy, it is crucial to prioritize high-benefit restored areas. Based on these considerations, the basic idea of MRELS is to optimize the restoration process by adjusting the restored areas while conserving the UAV's energy. This adjustment aims to maximize the total restoration areas achieved by the UAV. The MRELS procedure follows these steps:

Step 1 Identify the restored areas in the elite solution with the lowest energy consumption by the UAV.

Step 2 Increase the number of unit circles restored in these areas according to the corresponding UAV trajectory sequence.

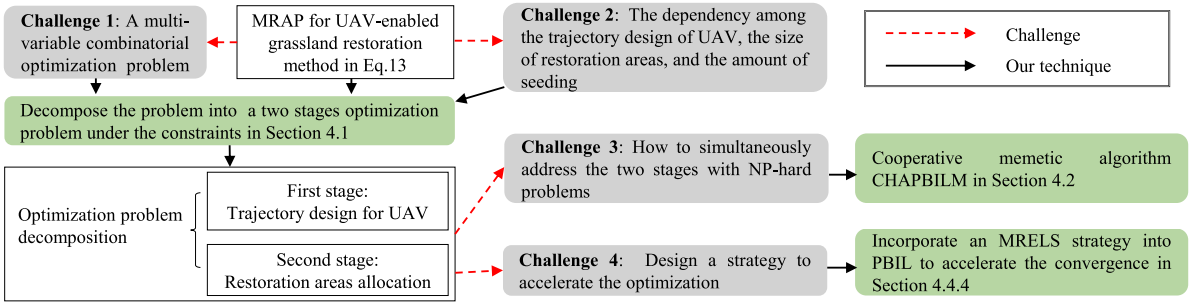

Fig. 3. Challenges and our techniques adopted in this study.

Step 3 For each feasible increase in the number of unit circles restored in an area, verify if the total restoration areas can be expanded without violating any constraints. If the increase is successful and adheres to the constraints, it is accepted as a valid adjustment.

Step 4 Repeat the above steps until all feasible restored areas have been examined and adjusted.

4.5. Computational complexity of CHAPBILM

The computational complexity of CHAPBILM can be analyzed as follows:

1. Initialization: The process of initializing solutions has a computational complexity of $O(N\times(NB+NP))$. This is because NB UAV paths and NP possible restoration area vectors are randomly generated.
2. Objective function evaluation: The computational complexity of evaluating the objective function is $O(NP\times N)$. This involves assessing the fitness of NP possible restoration area vectors for N restored areas.
3. UAV path generation: At each iteration of CHAPBILM, generating a new UAV path has a computational complexity of $O(NB\times N)$. This is done using the variable neighborhood operation.
4. Restoration area generation: The computational complexity of generating possible restoration areas is $O(NB\times(NP\times N))$. This involves generating NP possible restoration area vectors for NB UAV paths, considering N restored areas.
5. Objective function evaluation (again): The computational complexity of evaluating the objective function after generating new restoration areas is $O(NB\times(NP\times N))$. This entails assessing the fitness of the new restoration area vectors for NB UAV paths.
6. MRELS: The computational complexity of performing the MRELS local research strategy is $O(SP\times N)$, where SP is the number of solutions in the superior sub-population.

Therefore, the overall computational complexity of CHAPBILM is roughly $O(g_{max}\times(NB\times(NP\times N)))$, where g_{max} is the maximum number of iterations. The computational complexity of CHAPBILM depends on the neighborhood size of the generated paths NB, the number of restored areas N, and the population size NP.

4.6. Discussion

Fig. 3 provides a summary of the challenges addressed in this study and the techniques employed to tackle them. To overcome challenges 1 and 2, the MRAP of UAV-enabled grassland restoration method (13) is initially decomposed into a two-stage optimization problem while considering the constraints. Subsequently, a novel cooperative memetic algorithm called CHAPBILM is proposed to address challenges 3 and 4. Moreover, to enhance convergence and tackle challenge 4, an MRELS strategy is integrated into the variant PBIL. By implementing these techniques, the study aims to obtain the optimal UAV trajectory and the optimal total restoration areas.

5. Simulation studies

In this section, we present simulation evaluations conducted to assess the effectiveness of the proposed model and the cooperative optimization solution approach for the MRAP.

5.1. Simulation settings

The simulations were carried out on a workstation equipped with an AMD Ryzen Threadripper 3970X 32-Core CPU running at 3.79 GHz, 192 GB RAM, and operating on Windows 10. All simulation programs were developed using Python 3.9. The performance of the algorithm was evaluated using randomly generated test instances. It is important to mention that, for simplicity, all variables in this work were assigned uniform units.

5.1.1. Instance generation

To evaluate the effectiveness of our proposed model and algorithm, simulations were conducted on six different sizes of grassland areas. The area sizes ranged from 500 × 500 up to 1000 × 1000.[2] In each scenario, there were 15 degraded areas with varying degrees of degradation $l_i \in (0,1)$. The coordinates of the degraded areas were randomly generated within the given grassland area sizes. The base stations for all instances were located at coordinates $(0,0)$.

The number of unit circles restored σ_i for each degraded area on the grasslands varied from 10 to 35 in steps of 5 for all scenarios. The initial energy of UAV E_{max} varies from 1.36×10^7 to 3.64×10^7 in steps of 4.55×10^6 corresponding to the size of the grassland areas in each scenario. It is important to note that all the variables mentioned above followed a uniform distribution.

5.1.2. Compared algorithms

On the one hand, to verify the effectiveness of CHAPBILM for the MRAP, it is compared with another cooperative memetic algorithm, called CHAILS, in the six given scenarios. CHAILS is composed by our designed heuristic algorithm and an iterated local search (ILS) with MRELS operator. The ILS (Lourenço et al., 2003) merges an improvement heuristic operator within an iterative process to generate a sequence of solutions.

On the other hand, to further investigate the effectiveness of cooperative memetic algorithms for solving the problem, noncooperative algorithms are employed for comparison with CHAPBILM and CHAILS. In these noncooperative optimization algorithms, the trajectory design of the UAV and the allocation of restoration areas for each solution are obtained separately, in contrast to the nested structure of CHAPBILM and CHAILS. To be specific, Specifically, our designed heuristic

[2] In this work, all instances are defined in the 2D space, and the distance between two restored areas v_i and v_j is calculated using the Euclidean distance.

Table 2
Parameter settings of algorithm and model.

Parameter	Description	Value
NB	Neighborhood size of the generated path	36
gen_{max}	Maximum number generation	91
NP	Population size of variant PBIL	10
T_{max}	Maximum iteration number of variant PBIL	80
α	Learning rate	0.2
θ	Proportion of elite solution	30%
η	A positive parameter with energy consumption	1×10^5
γ	A positive parameter with grassland environment	2
e_{ap}	Energy consumption of UAV carrying the hyper-spectral camera for the aerial photography in each unit circle σ_i.	2×10^4

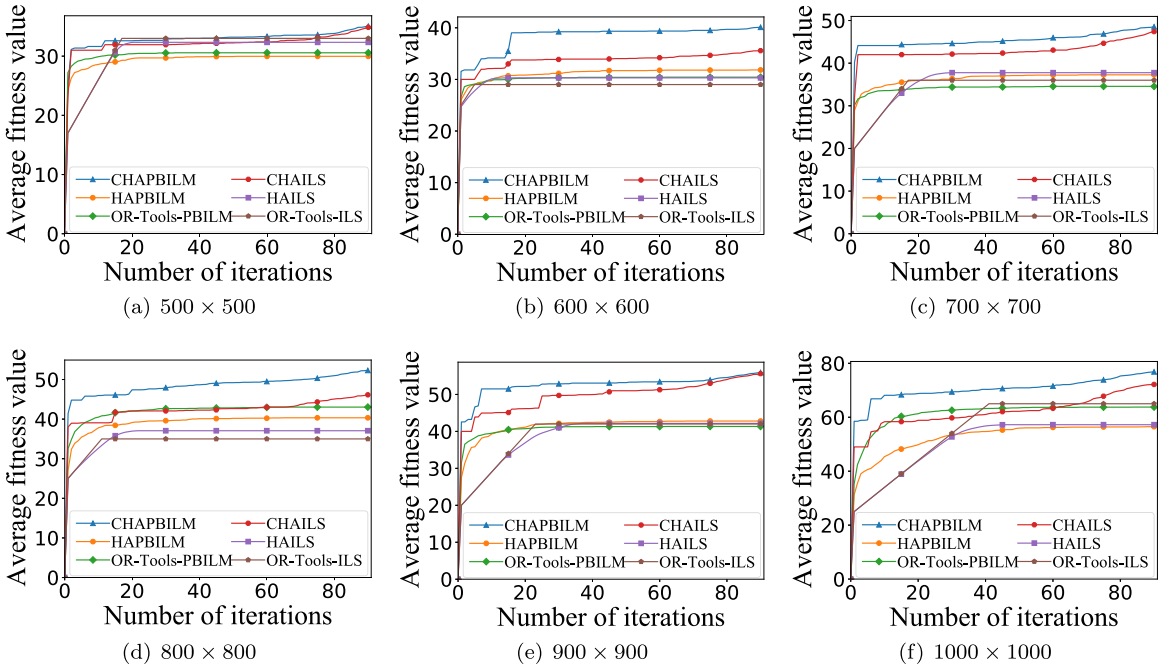

Fig. 4. Average convergence of cooperative and noncooperative optimization algorithms in six different scenarios. The CHAPBILM is the proposed algorithm in this work, and other algorithms are the comparative algorithms.

algorithm and Google (2021) OR-Tools[3] are respectively used for UAV trajectory design, while a variant of the PBIL and ILS with MRELS are respectively used to achieve optimal restoration area allocation. This results in four noncooperative algorithms for comparison: HA-PBILM, HA-ILS, OR-Tools-PBILM, and OR-Tools-ILS. It is important to note that OR-Tools, as an application programming interface (API), cannot directly solve the problem within the framework of cooperative optimization. Furthermore, OR-Tools is not suitable for solving the optimal restoration area allocation problem due to the presence of complicated nonlinear constraints in the optimization problem. Both OR-Tools-PBILM and CHAPBILM use a variant of PBIL to obtain the optimal restoration area allocation, but the difference lies in the optimization of the UAV's trajectory. OR-Tools is used in OR-Tools-PBILM to optimize the UAV's trajectory, while our designed heuristic algorithm is used in CHAPBILM. Additionally, both HA-ILS and CHAPBILM adopt the HA algorithm to obtain the UAV's trajectory, but HA-ILS utilizes ILS with MRELS instead of the variant PBIL algorithm to obtain the optimal restoration area allocation. The parameter settings for the variant PBIL in OR-Tools-PBILM are the same as those used in CHAPBILM.

[3] OR-Tools is open source software for combinatorial optimization, tuned for tackling the world's toughest problems in vehicle routing, flows, integer and linear programming, and constraint programming.

5.1.3. Parameter settings

In CHAPBILM, the neighborhood size NB of the generated path is 36 and the maximum number generation gen_{max} is set to 91. The population size and maximum iteration number of variant PBIL are respectively set to $NP = 10$ and $T_{max} = 80$. The learning rate and the proportion of elite solution are respectively set to $\alpha = 0.2$ and $\theta = 30\%$. To eliminate the influence of randomness on the simulation results as much as possible, each algorithm is independently executed 30 times in each scenario. The average value of these 30 runs is taken as the simulation results, ensuring a more reliable assessment of the algorithm's performance.

In the initial phase of ILS, the elements of the solution represent the number of unit circles restored σ_i for each degraded area on grasslands. The size of the grassland areas varies from 20% to 10% in decreasing steps of 5% at intervals of 2 for all the scenarios.

In the system model described in Section 3, the parameters of UAV are set as follows, based on the values used in Dorling et al. (2017): $M = 1.5$, $g = 9.8$, $\rho = 1.024$, $\varsigma = 0.2$, and $h = 6$. The parameters of energy consumption model for UAV in Section 3.2 are set to $\eta = 1\times10^5$, $\gamma = 2$, and $e_{ap} = 2\times10^4$.

The detailed parameter settings of algorithm and system model are summarized in Table 2.

Table 3
Comparison of solution results for cooperative and noncooperative optimization algorithms in six given grasslands.

Scenario	Cooperative optimization algorithms						Noncooperative optimization algorithms											
	CHAPBILM			CHAILS			HA-PBILM			HA-ILS			OR-Tools-PBILM			OR-Tools-ILS		
	Best	Avg	SD	Best	Avg	SD	Best	Avg	SD	Best	Avg	SD	Best	Avg	SD	Best	Avg	SD
500 × 500	**37**	**35**	1.00	**37**	**35**	0.88	35	30	2.83	36	32	2.18	33	31	1.09	33	33	0
600 × 600	**41**	**40**	0.54	36	36	0.50	37	32	2.92	35	30	3.42	33	30	1.56	29	29	0
700 × 700	**52**	**49**	1.36	49	47	1.11	47	37	5.32	49	38	5.94	38	35	2.09	36	36	0
800 × 800	**54**	**52**	1.04	50	46	2.40	49	40	5.77	46	37	5.67	49	43	4.39	35	35	0
900 × 900	58	**56**	1.24	**59**	**56**	1.40	57	43	7.02	56	42	8.04	46	41	3.14	42	42	0
1000 × 1000	**79**	**77**	1.13	75	72	1.44	74	57	10.94	70	57	6.81	73	64	6.90	65	65	0

Standard deviation is abbreviated as SD and average value is abbreviated as Avg.
Boldface value indicates better values among these algorithms.
All average value is rounded.

Table 4
Statistical test for Table 3.

Algorithm pairs	p-value					
	500 × 500	600 × 600	700 × 700	800 × 800	900 × 900	1000 × 1000
CHAPBILM *vs.* CHAILS	0.4689(*l*)	0.0000	0.0029	0.0000	0.2407(*l*)	0.0000
CHAPBILM *vs.* HA-PBILM	0.0000	0.0000	0.0000	0.0000	0.0000	0.0000
CHAPBILM *vs.* HA-ILS	0.0000	0.0000	0.0000	0.0000	0.0000	0.0000
CHAPBILM *vs.* OR-Tools-PBILM	0.0000	0.0000	0.0000	0.0000	0.0000	0.0000
CHAPBILM *vs.* OR-Tools-ILS	0.0000	0.0000	0.0000	0.0000	0.0000	0.0000
CHAILS *vs.* HA-PBILM	0.0000	0.0000	0.0000	0.0000	0.0000	0.0000
CHAILS *vs.* HA-ILS	0.0000	0.0000	0.0000	0.0000	0.0000	0.0000
CHAILS *vs.* OR-Tools-PBILM	0.0000	0.0000	0.0000	0.0021	0.0000	0.0000
CHAILS *vs.* OR-Tools-ILS	0.0000	0.0000	0.0000	0.0000	0.0000	0.0000

The Wilcoxon rank-sum test with significance level p is 0.05 and *l* indicates that the statistical result is nonsignificant.

5.2. Simulation results

5.2.1. Comparison of solution results for cooperative and noncooperative optimization algorithms

Fig. 4 illustrates the average convergence of cooperative and noncooperative optimization algorithms across six distinct scenarios, based on 30 independent runs. The results indicate that both cooperative optimization algorithms, CHAPBILM and CHAILS, consistently achieve higher-quality solutions compared to the four noncooperative optimization algorithms in all scenarios, although the convergence speed of noncooperative optimization algorithms is faster than that those under most scenarios. These findings suggest that jointly optimizing the UAV trajectory design and restoration areas allocation problem, as UAV in CHAPBILM, proves to be an effective solution for the MRAP.

Table 3 displays the solution results obtained from both cooperative and noncooperative optimization algorithms across six different scenarios. It is clear that with the increasing size of grassland areas, these two cooperative optimization algorithms shown on the gray background in Table 3 are significantly better than these four noncooperative optimization algorithms in terms of the best value and average value in all scenarios. Specifically from Table 8, it can be seen that when the size of grassland areas ranges from 500 × 500 to 1000 × 1000, the percentage improvement of solution results for CHAPBILM against other noncooperative optimization algorithms can achieve a maximum increase of 17.02%, 38.28%, 40.38%, 49.43%, and 35.98%, respectively. Furthermore, except for the scenarios of 500 × 500 and 900 × 900, CHAPBILM performs better than CHAILS with respect of the best value and average value in Table 3. All comparisons are confirmed by the nonparametric Wilcoxon rank-sum test with significance level $p = 0.05$. The statistical results presented in Table 4 show that the $p-$ values are all less than 0.05 except for the scenarios of 500 × 500 and 900 × 900, indicating that the observed differences are statistically significant.

Moreover, when the restoration areas reach the maximum by the UAV in a restoration process, the optimal path and the shortest path for the UAV are displayed in Table 5 and Fig. 5, respectively, for each of the six different scenarios. The results reveal that both the shortest path and the optimal path for the MRAP are distinct. This finding affirms the interdependence between the UAV trajectory design and the allocation of restoration areas.

The aforementioned results can be further explained as follows. In noncooperative optimization algorithms, the UAV trajectory design and restoration areas allocation are generated independently, which gives rise to two issues. On the one hand, when the shortest UAV trajectory is generated, the static trajectory cannot be adjusted adaptively with the dynamically changing restoration areas, so that the maximum restoration area is solely determined by the shortest UAV trajectory. This means that the trajectory planning of the UAV in noncooperative optimization algorithms remains unaffected by the maximum restoration area. On the other hand, it is very possible that the noncooperative optimization algorithms obtain one solution consisting of a "good" UAV trajectory yet a "bad" maximum restoration area. It is viewed that unpromising solution as a whole, which cannot accurately reflect the dependency relationship between UAV trajectory design and restoration area allocation. On the contrary, our proposed cooperative optimization algorithms fully consider the interdependencies between them and can obtain the corresponding optimal allocation of restoration areas, resulting that the promising UAV trajectory can be maintained. Furthermore, the results also indicate that the shortest path for UAV flight may not lead to the maximum restoration area. This finding further confirms the capabilities and efficiency of our proposed cooperative optimization algorithms for the MRAP.

5.2.2. Effectiveness of MRELS for cooperative and noncooperative optimization algorithms

To verify the advantage of the designed MRELS strategy, the performance comparison results are demonstrated in Fig. 6 and Table 6. The findings indicate that the MRELS strategy not only accelerates the convergence of both cooperative and noncooperative optimization algorithms but also achieves better high-quality solutions. Table 8 reveals that the average value of CHAPBILM can improve by up to 43.15% compared with CHAPBIL in the scenario of 1000 × 1000. In particular, the effectiveness of the MRELS strategy becomes more pronounced as the size of the grassland areas increases. This is due to the fact that the MRELS strategy focuses on maximizing restoration areas by

Table 5
Comparison of the optimal path and the shortest path in six given grasslands.

Scenario	Path	
500 × 500	Shortest path	0 → 14 → 3 → 2 → 10 → 13 → 8 → 7 → 15 → 5 → 9 → 4 → 12 → 1 → 11 → 6 → 0
	Optimal path	0 → 6 → 11 → 1 → 12 → 4 → 2 → 3 → 14 → 10 → 15 → 13 → 7 → 5 → 9 → 8 → 0
600 × 600	Shortest path	0 → 3 → 13 → 5 → 11 → 12 → 8 → 2 → 15 → 6 → 9 → 7 → 4 → 14 → 1 → 10 → 0
	Optimal path	0 → 10 → 1 → 4 → 14 → 7 → 12 → 6 → 13 → 3 → 11 → 5 → 15 → 2 → 8 → 9 → 0
700 × 700	Shortest path	0 → 12 → 2 → 7 → 9 → 8 → 4 → 15 → 6 → 14 → 13 → 3 → 11 → 1 → 5 → 10 → 0
	Optimal path	0 → 5 → 10 → 11 → 3 → 15 → 13 → 14 → 4 → 1 → 8 → 7 → 6 → 12 → 2 → 9 → 0
800 × 800	Shortest path	0 → 4 → 7 → 11 → 10 → 1 → 15 → 12 → 8 → 2 → 6 → 14 → 3 → 9 → 13 → 5 → 0
	Optimal path	0 → 5 → 13 → 7 → 4 → 8 → 6 → 11 → 14 → 10 → 3 → 2 → 12 → 1 → 15 → 9 → 0
900 × 900	Shortest path	0 → 8 → 13 → 5 → 12 → 2 → 11 → 6 → 15 → 14 → 7 → 1 → 9 → 3 → 4 → 10 → 0
	Optimal path	0 → 4 → 10 → 1 → 7 → 3 → 8 → 13 → 15 → 6 → 12 → 2 → 11 → 5 → 14 → 9 → 0
1000 × 1000	Shortest path	0 → 12 → 11 → 8 → 7 → 10 → 5 → 1 → 3 → 15 → 6 → 14 → 2 → 9 → 13 → 4 → 0
	Optimal path	0 → 4 → 12 → 11 → 10 → 8 → 1 → 15 → 3 → 13 → 5 → 7 → 2 → 6 → 14 → 9 → 0

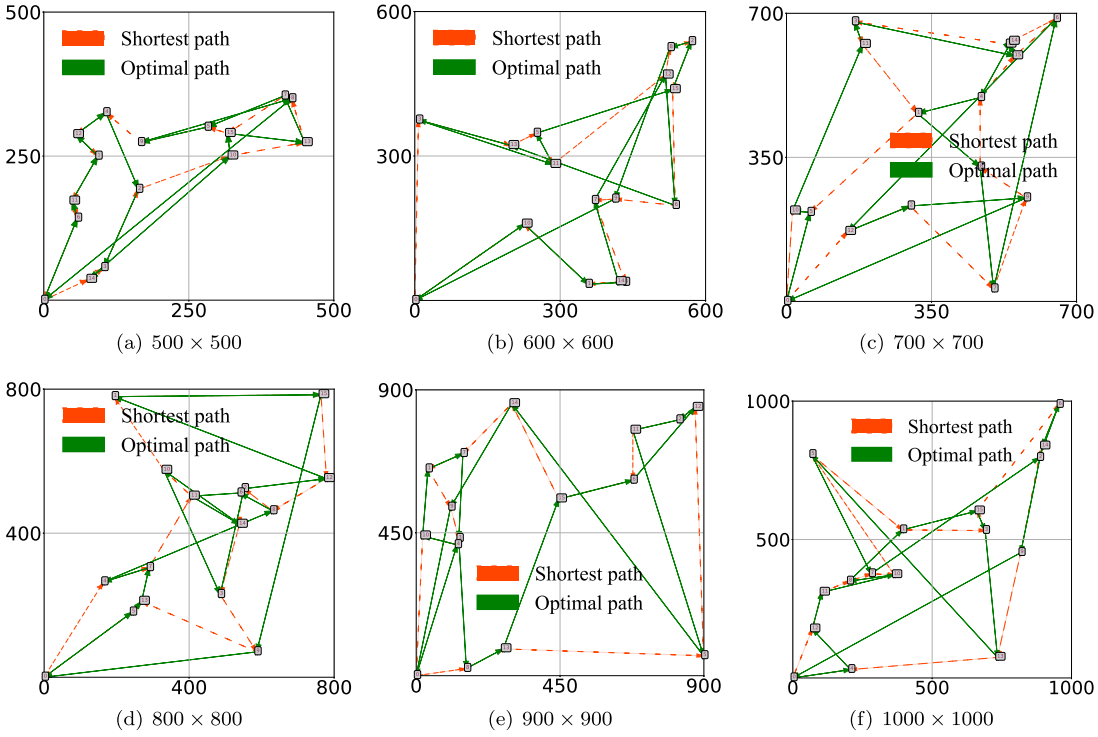

Fig. 5. Visualization of the optimal path and the shortest path in six different scenarios.

optimizing the UAV's residual energy. The energy consumption of the UAV depends on factors such as the degradation degree and the number of unit circles restored in each area, as well as the distance and weight of grass seeds carried between restored areas. The MRELS strategy prioritizes the restoration of unit circles in areas with higher residual energy, thereby maximizing the overall restoration areas. Moreover, the statistical test is also used to confirm the comparison results. Table 7 shows that the $p-$ values with MRELS are statistically significant.

6. Conclusion

This work focused on addressing the multivariable combinatorial optimization problem of MRAP (UAV-enabled grassland restoration) in a single trip. It was the first study to tackle this problem, which involved jointly optimizing the UAV trajectory design and restoration areas allocation. The objective was to maximize the restoration area while considering constraints related to UAV energy, grass seed weight, the number of restored areas, and their respective sizes. The problem naturally decomposed into two stages: UAV trajectory design and restoration areas allocation. Each subproblem within these stages was NP-hard. To address this challenge, a novel cooperative memetic algorithm called CHAPBILM was proposed, ensuring that the dependence between the stages was not overlooked. In this framework, an efficient heuristic algorithm with move operators was employed to design the optimal UAV trajectory. Additionally, the variant of PBIL integrated with the energy-sensitive MRELS strategy was utilized to identify the maximum restoration area corresponding to the optimal UAV trajectory. The two algorithms worked cooperatively to obtain the optimal solution. The simulation results demonstrated that the cooperative memetic algorithm outperformed noncooperative optimization algorithms. This finding confirmed the dependency relationship between UAV trajectory design and restoration areas allocation. The results highlighted the effectiveness of the formulated model in capturing the characteristics of the MRAP for UAV-enabled grassland restoration method.

The UAV-enabled grassland restoration method, despite restoring only a subset of degraded areas, holds great potential for enhancing

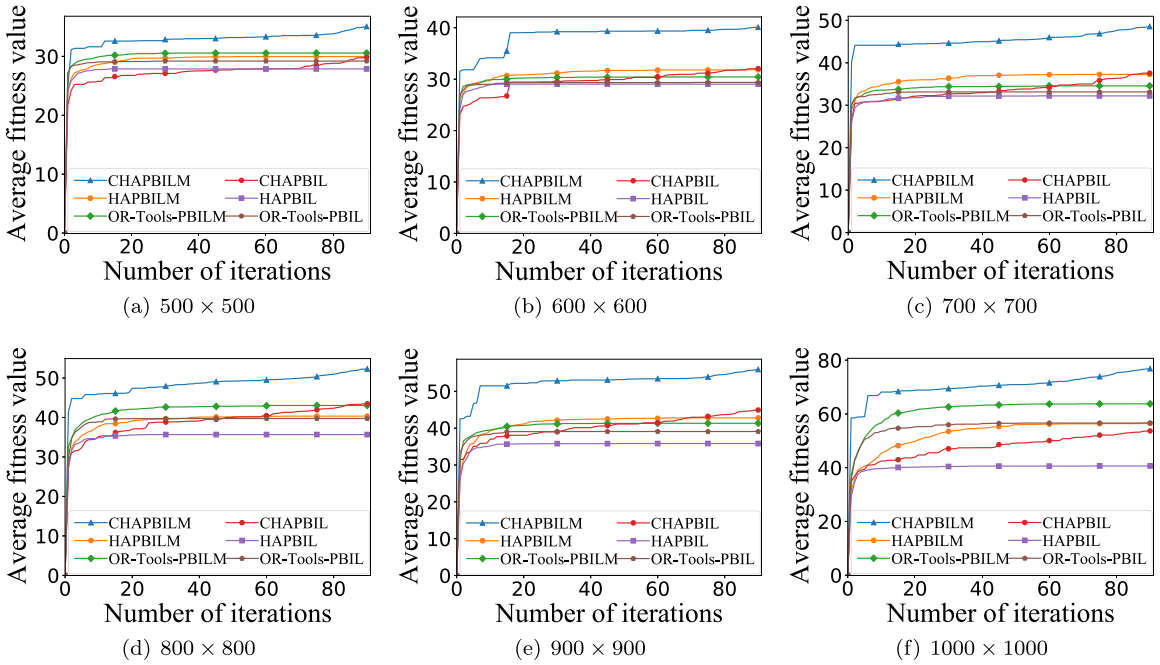

Fig. 6. Average performance of cooperative and noncooperative optimization algorithms with and without local search in six different scenarios.

Table 6
Comparison of solution results for cooperative and noncooperative optimization algorithms with and without local search in six given grasslands.

Scenario	Cooperative optimization algorithms						Noncooperative optimization algorithms											
	CHAPBILM			CHAPBIL			HA-PBILM			HA-PBIL			OR-Tools-PBILM			OR-Tools-PBIL		
	Best	Avg	SD	Best	Avg	SD	Best	Avg	SD	Best	Avg	SD	Best	Avg	SD	Best	Avg	SD
500 × 500	37	35	1.00	35	30	2.48	35	30	2.83	33	28	2.00	33	31	1.09	31	29	0.60
600 × 600	41	40	0.54	38	32	2.52	37	32	2.92	36	29	3.21	33	30	1.56	33	29	1.80
700 × 700	52	49	1.36	47	38	4.62	47	37	5.32	42	32	4.13	38	35	2.09	36	33	1.98
800 × 800	54	52	1.04	49	43	3.12	49	40	5.77	48	36	5.87	49	43	4.39	47	40	5.62
900 × 900	58	56	1.24	53	45	3.57	57	43	7.02	52	36	6.18	46	41	3.14	45	39	3.99
1000 × 1000	79	77	1.13	75	54	9.54	74	57	10.94	76	41	11.30	73	64	6.90	69	57	10.25

Standard deviation is abbreviated as SD and average value is abbreviated as Avg.
The value with gray background shows the results with local search.
All averages are rounded.

Table 7
Statistical test for Table 6.

Algorithm pairs	*p*-value					
	500 × 500	600 × 600	700 × 700	800 × 800	900 × 900	1000 × 1000
CHAPBILM *vs.* CHAPBIL	0.0000	0.0000	0.0000	0.0000	0.0000	0.0000
CHAPBILM *vs.* HA-PBILM	0.0000	0.0000	0.0000	0.0000	0.0000	0.0000
CHAPBILM *vs.* HA-PBILS	0.0000	0.0000	0.0000	0.0000	0.0000	0.0000
CHAPBILM *vs.* OR-Tools-PBILM	0.0000	0.0000	0.0000	0.0000	0.0000	0.0000
CHAPBILM *vs.* OR-Tools-PBIL	0.0000	0.0000	0.0000	0.0000	0.0000	0.0000
CHAPBIL *vs.* HA-PBILM	0.3068(*l*)	0.8117(*l*)	0.4059(*l*)	0.0055	0.0734(*l*)	0.0343
CHAPBIL *vs.* HA-PBIL	0.0187	0.0000	0.0000	0.0000	0.0000	0.0015
CHAPBIL *vs.* OR-Tools-PBILM	0.2187(*l*)	0.0195	0.0296	0.7269(*l*)	0.0003	0.0001
CHAPBIL *vs.* OR-Tools-PBIL	0.2453(*l*)	0.0000	0.0004	0.0052	0.0000	0.6785(*l*)

The Wilcoxon rank-sum test with significance level p is 0.05 and l indicates that the statistical result is nonsignificant.

grassland intelligence and significantly reducing restoration costs. It is considered a promising approach for future grassland ecological protection. Therefore, it is worthwhile to further investigate and explore the UAV-enabled grassland restoration method to preserve the ecological environment of grasslands. The model and solution presented in this work can be extended to other related fields, including UAV earthquake rescue and air delivery. In future research, we plan to incorporate the UAV dynamic model, including velocity considerations, as well as explore online optimization algorithms. Additionally, we aim to extend the method to address larger grassland degradation areas with obstacles in 3D terrain, taking inspiration from the works of Yang et al. (2015) and Fan et al. (2022).

Table 8
Percentage improvement of solution results for CHAPBILM compared with other algorithms in six given grasslands.

Scenario	CHAPBIL	CHAILS	HA-PBILM	HA-PBIL	HA-ILS	OR-Tools-PBILM	OR-Tools-PBIL	OR-Tools-ILS
500 × 500	17.57%	0.57%	17.02%	25.83%	8.48%	14.72%	20.10%	6.27%
600 × 600	25.04%	12.74%	25.98%	38.13%	32.34%	31.78%	36.53%	38.28%
700 × 700	29.17%	2.38%	30.21%	50.71%	28.49%	40.38%	46.48%	34.81%
800 × 800	20.31%	13.38%	29.68%	46.62%	41.08%	21.54%	31.64%	49.43%
900 × 900	24.48%	0.54%	30.68%	56.10%	32.63%	35.33%	43.04%	33.17%
1000 × 1000	43.15%	6.45%	35.98%	89.10%	34.25%	20.48%	35.67%	18.20%

The value with gray background shows the results with local search.
The percentage improvement of solution results is calculated based on the average of original data without rounding.

CRediT authorship contribution statement

Dongbin Jiao: Writing – original draft, Validation, Resources, Methodology, Investigation, Conceptualization. **Lingyu Wang:** Visualization, Validation, Software, Data curation. **Peng Yang:** Writing – review & editing, Validation, Methodology, Investigation. **Weibo Yang:** Validation, Investigation. **Yu Peng:** Software, Data curation. **Zhanhuan Shang:** Validation, Investigation. **Fengyuan Ren:** Writing – review & editing, Supervision, Project administration.

Declaration of competing interest

The authors declare that they have no known competing financial interests or personal relationships that could have appeared to influence the work reported in this paper.

Data availability

Data will be made available on request.

Acknowledgments

This work was supported in part by National Natural Science Foundation of China (Grant No. 62176109, U21A20183, 62272210, and 31870433), the Fundamental Research Funds for the Central Universities, PR China (Grant No. lzujbky-2021-2, CHD300102223109), the Natural Science Foundation of Gansu Province, China (Grant No. 20JR10RA640), the Guangdong Provincial Key Laboratory, PR China (Grant No. 2020B121201001), and the Hui-Chun Chin and Tsung-Dao Lee Chinese Undergraduate Research Endowment, PR China (Grant No. LZU-JZH2514). The authors would like to thank Dr. G. Zhang, Mr. Z. Wang, Dr. S. Liu, Dr. S. Li, Prof. K. Tang, and Prof. K. Li for kind help and valuable discussions. We also thank the anonymous referees for their insightful comments and helpful suggestions which significantly improve the manuscript's quality.

References

Aggarwal, S., Kumar, N., 2020. Path planning techniques for unmanned aerial vehicles: A review, solutions, and challenges. Comput. Commun. 149, 270–299.
Angelo, J.S., Barbosa, H.J., 2015. A study on the use of heuristics to solve a bilevel programming problem. Int. Trans. Oper. Res. 22 (5), 861–882.
Azadeh, S.S., Bierlaire, M., Maknoon, M., 2019. A two-stage route optimization algorithm for light aircraft transport systems. Transp. Res. C 100, 259–273.
Bai, Y., Ma, L., Degen, A.A., Rafiq, M.K., Kuzyakov, Y., Zhao, J., Zhang, R., Zhang, T., Wang, W., Li, X., et al., 2020. Long-term active restoration of extremely degraded alpine grassland accelerated turnover and increased stability of soil carbon. Global Change Biol. 26 (12), 7217–7228.
Baluja, S., 1994. Population-Based Incremental Learning: A Method for Integrating Genetic Search Based Function Optimization and Competitive Learning. Technical Report CMU-CS-94-163, Carnegie Mellon University, Pittsburgh, PA.
Basiri, A., Mariani, V., Silano, G., Aatif, M., Iannelli, L., Glielmo, L., 2022. A survey on the application of path-planning algorithms for multi-rotor UAVs in precision agriculture. J. Navig. 75 (2), 364–383.
Blackburn, R.C., Barber, N.A., Farrell, A.K., Buscaglia, R., Jones, H.P., 2021. Monitoring ecological characteristics of a tallgrass prairie using an unmanned aerial vehicle. Restor. Ecol. 29, e13339.
Bräysy, O., Gendreau, M., 2005. Vehicle routing problem with time windows, Part I: Route construction and local search algorithms. Transp. Sci. 39 (1), 104–118.
Buters, T., Belton, D., Cross, A., 2019. Seed and seedling detection using unmanned aerial vehicles and automated image classification in the monitoring of ecological recovery. Drones 3 (3), 53.
Chapin, F.S., Sala, O.E., Huber-Sannwald, E., 2013. Global Biodiversity in a Changing Environment: Scenarios for the 21st Century. Vol. 152, Springer Science & Business Media.
Chiang, W.-C., Li, Y., Shang, J., Urban, T.L., 2019. Impact of drone delivery on sustainability and cost: Realizing the UAV potential through vehicle routing optimization. Appl. Energy 242, 1164–1175.
Colson, B., Marcotte, P., Savard, G., 2007. An overview of bilevel optimization. Ann. Oper. Res. 153 (1), 235–256.
Dass, P., Houlton, B.Z., Wang, Y., Warlind, D., 2018. Grasslands may be more reliable carbon sinks than forests in california. Environ. Res. Lett. 13 (7), 074027.
Dorling, K., Heinrichs, J., Messier, G.G., Magierowski, S., 2017. Vehicle routing problems for drone delivery. IEEE Trans. Syst. Man Cybern.: Syst. 47 (1), 70–85.
Elliott, S., 2016. The potential for automating assisted natural regeneration of tropical forest ecosystems. Biotropica 48 (6), 825–833.
Faiçal, B.S., Freitas, H., Gomes, P.H., Mano, L.Y., Pessin, G., de Carvalho, A.C., Krishnamachari, B., Ueyama, J., 2017. An adaptive approach for UAV-based pesticide spraying in dynamic environments. Comput. Electron. Agric. 138, 210–223.
Fan, J., Chen, X., Wang, Y., Chen, X., 2022. UAV trajectory planning in cluttered environments based on PF-RRT algorithm with goal-biased strategy. Eng. Appl. Artif. Intell. 114, 105182.
Fang, C., Han, Z., Wang, W., Zio, E., 2023. Routing UAVs in landslides monitoring: A neural network heuristic for team orienteering with mandatory visits. Transp. Res. E 175, 103172.
Feng, L., Ong, Y.-S., Tan, A.-H., Tsang, I.W., 2015. Memes as building blocks: a case study on evolutionary optimization+ transfer learning for routing problems. Memet. Comput. 7 (3), 159–180.
Fidanova, S., 2021. Multiple knapsack problem. In: Ant Colony Optimization and Applications. Springer, pp. 9–18.
Fleszar, K., 2022. A branch-and-bound algorithm for the quadratic multiple knapsack problem. European J. Oper. Res. 298 (1), 89–98.
Freitag, M., Klaus, V.H., Bolliger, R., Hamer, U., Kleinebecker, T., Prati, D., Schäfer, D., Hölzel, N., 2021. Restoration of plant diversity in permanent grassland by seeding: Assessing the limiting factors along land-use gradients. J. Appl. Ecol. 58 (8), 1681–1692.
Gann, G.D., McDonald, T., Walder, B., Aronson, J., Nelson, C.R., Jonson, J., Hallett, J.G., Eisenberg, C., Guariguata, M.R., Liu, J., et al., 2019. International principles and standards for the practice of ecological restoration. Restor. Ecol. 27, S1–S46.
Gibson, D.J., 2009. Grasses and Grassland Ecology. Oxford University Press.
Gong, M., Chen, C., Xie, Y., Wang, S., 2020. Community preserving network embedding based on memetic algorithm. IEEE Trans. Emerg. Top. Comput. Intell. 4 (2), 108–118.
Google, 2021. OR-Tools. https://developers.google.com/optimization.
Guo, Y., Liu, C., Coombes, M., 2021. Spraying coverage path planning for agriculture unmanned aerial vehicles. In: 2021 26th International Conference on Automation and Computing. ICAC, IEEE, pp. 1–6.
Hong, L., Wang, Y., Du, Y., Chen, X., Zheng, Y., 2021. UAV search-and-rescue planning using an adaptive memetic algorithm. Front. Inf. Technol. Electron. Eng. 22 (11), 1477–1491.
Huang, X., 2004. Cooperative optimization for solving large scale combinatorial problems. In: Theory and Algorithms for Cooperative Systems. World Scientific, pp. 117–156.
Huang, X., Zhang, S., Luo, C., Li, W., Liao, Y., 2020. Design and experimentation of an aerial seeding system for rapeseed based on an air-assisted centralized metering device and a multi-rotor crop protection UAV. Appl. Sci. 10 (24), 8854.
Jiao, D., Ke, L., Yang, W., Li, J., 2017. An estimation of distribution algorithm based dynamic clustering approach for wireless sensor networks. Wirel. Pers. Commun. 97 (3), 4697–4727.
Kellerer, H., Pferschy, U., Pisinger, D., 2004. Multidimensional knapsack problems. In: Knapsack Problems. Springer, pp. 235–283.
Klaus, V.H., Schäfer, D., Kleinebecker, T., Fischer, M., Prati, D., Hölzel, N., 2016. Enriching plant diversity in grasslands by large-scale experimental sward disturbance and seed addition along gradients of land-use intensity. J. Plant Ecol. 10 (4), 581–591.

Li, W., Li, Y., Li, C., Huang, G., 2010. An inexact two-stage water management model for planning agricultural irrigation under uncertainty. Agricult. Water Manag. 97 (11), 1905–1914.

Librán-Embid, F., Klaus, F., Tscharntke, T., Grass, I., 2020. Unmanned aerial vehicles for biodiversity-friendly agricultural landscapes-a systematic review. Sci. Total Environ. 732, 139204.

Liu, S., Tang, K., Yao, X., 2021. Memetic search for vehicle routing with simultaneous pickup-delivery and time windows. Swarm Evol. Comput. 66, 100927.

Lourenço, H.R., Martin, O.C., Stützle, T., 2003. Iterated local search. In: Handbook of Metaheuristics. Springer, pp. 320–353.

Maini, P., Sundar, K., Singh, M., Rathinam, S., Sujit, P., 2019. Cooperative aerial–ground vehicle route planning with fuel constraints for coverage applications. IEEE Trans. Aerosp. Electron. Syst. 55 (6), 3016–3028.

Merz, P., 2000. Memetic Algorithms for Combinatorial Optimization Problems: Fitness Landscapes and Effective Search Strategies. (Ph.D. thesis). Department of Electrical Engineering and Computer Science, University of Siegen.

Mohan, M., Richardson, G., Gopan, G., Aghai, M.M., Bajaj, S., Galgamuwa, G., Vastaranta, M., Arachchige, P.S.P., Amorós, L., Corte, A.P.D., et al., 2021. UAV-supported forest regeneration: Current trends, challenges and implications. Remote Sens. 13 (13), 2596.

Ong, Y.-S., Lim, M.H., Chen, X., 2010. Research frontier-memetic computation—past, present & future. IEEE Comput. Intell. Mag. 5 (2), 24–31.

Palomino-Suarez, D., Pérez-Ruiz, A., 2020. Towards automatic UAV path planning in agriculture oversight activities. In: Proceedings of the Latin American Congress on Automation and Robotics. Springer, pp. 22–30.

Pedersen, S.M., Fountas, S., Sørensen, C.G., Van Evert, F.K., Blackmore, B.S., 2017. Robotic seeding: Economic perspectives. In: Precision Agriculture: Technology and Economic Perspectives. Springer, pp. 167–179.

Rajan, S., Sundar, K., Gautam, N., 2022. Routing problem for unmanned aerial vehicle patrolling missions–a progressive hedging algorithm. Comput. Oper. Res. 142, 105702.

Reinermann, S., Asam, S., Kuenzer, C., 2020. Remote sensing of grassland production and management — A review. Remote Sens. 12 (12), 1949.

Resch, M.C., Schütz, M., Ochoa-Hueso, R., Buchmann, N., Frey, B., Graf, U., van der Putten, W.H., Zimmermann, S., Risch, A.C., 2022. Long-term recovery of above- and belowground interactions in restored grasslands after topsoil removal and seed addition. J. Appl. Ecol. 59 (9), 2299–2308.

Reynolds, S., Frame, J., 2005. Grasslands: Developments, Opportunities, Perspectives. Science Publishers.

Rezoug, A., Bader-El-Den, M., Boughaci, D., 2018. Guided genetic algorithm for the multidimensional knapsack problem. Memet. Comput. 10 (1), 29–42.

Rossello, N.B., Carpio, R.F., Gasparri, A., Garone, E., 2022. Information-driven path planning for UAV with limited autonomy in large-scale field monitoring. IEEE Trans. Autom. Sci. Eng. 19 (3), 2450–2460.

Shakhatreh, H., Sawalmeh, A.H., Al-Fuqaha, A., Dou, Z., Almaita, E., Khalil, I., Othman, N.S., Khreishah, A., Guizani, M., 2019. Unmanned aerial vehicles (UAVs): A survey on civil applications and key research challenges. IEEE Access 7, 48572–48634.

Shivgan, R., Dong, Z., 2020. Energy-efficient drone coverage path planning using genetic algorithm. In: 2020 IEEE 21st International Conference on High Performance Switching and Routing. HPSR, IEEE, pp. 1–6.

Sinha, A., Malo, P., Deb, K., 2018. A review on bilevel optimization: from classical to evolutionary approaches and applications. IEEE Trans. Evol. Comput. 22 (2), 276–295.

Steffen, W., Richardson, K., Rockström, J., Cornell, S.E., Fetzer, I., Bennett, E.M., Biggs, R., Carpenter, S.R., De Vries, W., De Wit, C.A., et al., 2015. Planetary boundaries: Guiding human development on a changing planet. Science 347 (6223), 1259855.

Sun, Y., Yi, S., Hou, F., 2018. Unmanned aerial vehicle methods makes species composition monitoring easier in grasslands. Ecol. Indic. 95, 825–830.

Török, P., Brudvig, L.A., Kollmann, J., N Price, J., Tóthmérész, B., 2021. The present and future of grassland restoration. Restor. Ecol. 29, e13378.

Vasisht, D., Kapetanovic, Z., Won, J., Jin, X., Chandra, R., Sinha, S., Kapoor, A., Sudarshan, M., Stratman, S., 2017. Farmbeats: An IoT platform for data-driven agriculture. In: 14th USENIX Symposium on Networked Systems Design and Implementation NSDI 17. USENIX Association, Boston, MA, pp. 515–529.

Wang, W., Fang, C., Liu, T., 2022. Multiperiod unmanned aerial vehicles path planning with dynamic emergency priorities for geohazards monitoring. IEEE Trans. Ind. Inform. 18 (12), 8851–8859.

Wang, J.-j., Wang, L., 2021. A bi-population cooperative memetic algorithm for distributed hybrid flow-shop scheduling. IEEE Trans. Emerg. Top. Comput. Intell. 5 (6), 947–961.

Wang, L., Wang, S.-y., Xu, Y., 2012. An effective hybrid EDA-based algorithm for solving multidimensional knapsack problem. Expert Syst. Appl. 39 (5), 5593–5599.

Wang, J., Zhang, Y., Geng, L., Fuh, J.Y., Teo, S., 2015. A heuristic mission planning algorithm for heterogeneous tasks with heterogeneous UAVs. Unmanned Syst. 3 (03), 205–219.

Wang, H., Zhao, H., Wu, W., Xiong, J., Ma, D., Wei, J., 2019. Deployment algorithms of flying base stations: 5G and beyond with UAVs. IEEE Internet Things J. 6 (6), 10009–10027.

Xiang, T.-Z., Xia, G.-S., Zhang, L., 2019. Mini-unmanned aerial vehicle-based remote sensing: techniques, applications, and prospects. IEEE Geosci. Remote Sens. Mag. 7 (3), 29–63.

Yang, P., Tang, K., Lozano, J.A., Cao, X., 2015. Path planning for single unmanned aerial vehicle by separately evolving waypoints. IEEE Trans. Robot. 31 (5), 1130–1146.

Yang, P., Zhang, L., Liu, H., Li, G., 2024. Reducing idleness in financial cloud services via multi-objective evolutionary reinforcement learning based load balancer. Sci. China Inf. Sci. 67 (2), 120102.

Zhao, H., Wang, H., Wu, W., Wei, J., 2018. Deployment algorithms for UAV airborne networks toward on-demand coverage. IEEE J. Sel. Areas Commun. 36 (9), 2015–2031.